9470 *Inorg. Chem.* **2010**, *49*, 9470–9478
DOI: 10.1021/ic1011499

Inorganic Chemistry
Article

Brillouin Spectroscopy, Calculated Elastic and Bond Properties of $GaAsO_4$

Gopalkrishna M. Bhalerao, Olivier Cambon,* and Julien Haines

Institut Charles Gerhardt Montpellier, UMR-CNRS-UM2-ENSCM-UM1 5253, Université Montpellier 2, Equipe C2M, Place E. Bataillon, 34095 Montpellier, Cedex 5, France

Claire Levelut

Laboratoire des Colloides, des Verres et des Nanomatériaux, Université Montpellier 2, cc026, Place E. Bataillon, F-34095 Montpellier Cedex 5, France

Alain Mermet and Sergey Sirotkin

Laboratoire de Physico-Chimie des Matériaux Luminescents, Université de Lyon, UMR CNRS 5620, Université Claude Bernard Lyon 1, 69622 Villeurbanne Cedex, France

Bertrand Ménaert and Jérôme Debray

Institut Néel Grenoble, UPR-CNRS 2940, Département Matière Condensée Matériaux et Fonctions, 25 avenue des Martyrs, BP166, 38042 Grenoble Cedex 9, France

Isabelle Baraille, Clovis Darrigan, and Michel Rérat

Université de Pau et des Pays de l'Adour/CNRS UMR 5254, IPREM, 2 avenue du Président Angot, 64053 Pau, Cedex 9, France

Received June 8, 2010

Experimental and theoretical studies have been performed to demonstrate the high performance of the novel piezoelectric material $GaAsO_4$. Hydrothermally grown single crystals of α-quartz phase $GaAsO_4$ were studied by Brillouin spectroscopy to determine elastic constants. Experimentally obtained values of C_{11}, C_{66}, C_{33}, C_{44}, C_{14} and C_{12} are 59.32, 19.12, 103.54, 30.70, 1.7, and 21.1 GPa, respectively. Elastic and piezoelectric tensors were also calculated by a first principles method in this work, leading to a very good agreement with experimental results and confirming the values of elastic components obtained indirectly such as C_{14} and the negligible piezoelectric correction for C_{11}. The thermal behavior of the elastic constant corresponding to the [100] longitudinal L mode (C_{11}) was studied up to 1137 K to estimate potential piezoelectric performance. It was found that the thermal behavior is linear up to 1273 K which is just below the thermal decomposition temperature of 1303 K. High thermal stability can be linked to the higher polarizability of large cations Ga and As because of neighboring oxygen atoms. On the basis of thermal behavior, $GaAsO_4$ is a promising material for high temperature piezoelectric applications.

1. Introduction

Quartz is the most widely used material in piezoelectric applications. Its piezoelectric performance degrades above about 573 K, and it transforms to β-phase at 846 K.[1,2] Therefore quartz is not suitable for applications requiring high thermal stability or a high electro-mechanical coupling coefficient. Piezoelectric performance of the quartz homeotypes $A^{III}B^{V}O_4$ (A^{III} = B, Al, Ga, Fe and B^{V} = P, As) is predicted to be better than that of quartz. These materials belong to space groups $P3_121$ or $P3_221$, and the structure can

*To whom correspondence should be addressed. E-mail: ocambon@lpmc.univ-montp2.fr.

(1) Haines, J.; Cambon, O.; Keen, D. A.; Tucker, M. G.; Dove, M. T. *Appl. Phys. Lett.* **2002**, *81*, 2968.

(2) Cambon, O.; Haines, J.; Fraysse, G.; Keen, D. A.; Tucker, M. G. *J. Phys. IV* **2005**, *126*, 27.

Published on Web 09/16/2010

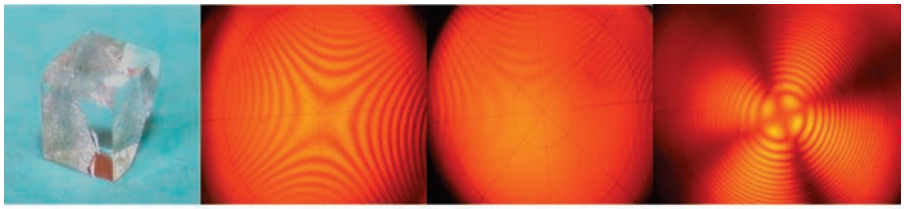

Figure 1. (a) $2 \times 2 \times 2$ mm cube cut from a $GaAsO_4$ single crystal with *X*, *Y*, and *Z* polished faces. (b, c, d): conoscopy of the *X*, *Y*, and *Z* faces. Optical axis is observed on the *Z*-face.

be described as a helical chain of alternating AO_4 and BO_4 tetrahedra along the *z*-axis. Piezoelectric properties in quartz homeotypes are related to distortion of the structure with respect to that of β-quartz. Structural parameters such as the intertetrahedral bridging angle θ ($A-O-B$) and the tetrahedral tilt angle δ quantify the distortion.[3] The latter is an order parameter for $\alpha-\beta$ transition and corresponds to the rotation of the tetrahedra about their 2-fold axes parallel to *x*. For α-quartz at room temperature, $\theta = 143.6°$, $\delta = 16.4°$ and for β-quartz at 848 K, $\theta = 153.3°$, $\delta = 0°$.[4] On this basis, structure−property relationships have been established between thermal stability, physical and piezoelectric properties, and the structural distortion in these materials.[5−14] Better thermal stability with respect to the $\alpha-\beta$ transition has been observed for materials having a greater structural distortion.[6] There is also a linear dependence between the electromechanical coupling coefficient and the structural distortion.[6]

$GaAsO_4$ has been found to have the most distorted structure and the highest electromechanical coupling coefficient ($k = 21\%$) in the quartz group.[15] The distortion determines the material's response to temperature and pressure.[6,14] Values of $\theta = 129.6°$, and $\delta = 26.9°$ for $GaAsO_4$ indicate that its structure is highly distorted.[7] Ab initio calculations with full optimization of geometry obtained in this work yield values which are in very good agreement with these experimental results.

No phase-transformation is observed on heating before thermal decomposition at about 1303 K.[15] High temperature X-ray diffraction studies have shown that the structural distortion does not vary significantly as a function of temperature.[15] Hence, $GaAsO_4$ has high potential for high temperature piezoelectric applications.

It is necessary to study experimentally the piezoelectric properties to establish its suitability for possible applications. Piezoelectric properties, for example the *n*th harmonic of resonance frequency f_n depends on the elastic constant C_{ij} of the crystal as follows $f_n = (n/2t)(C_{ij}/\rho)^{1/2}$, where ρ is density and *t* the thickness of specimen plate.[16] Hence, the piezoelectric behavior can be predicted based on the elastic constants of the material under consideration. Although several structural and crystallographic studies on $GaAsO_4$ have been made, direct measurements of piezoelectric properties by the frequency resonance method are limited to an AT-rotated cut ($-6.3°$ from *Y* plane for $GaAsO_4$),[15] with the values of $k = 21\%$ and elastic constant $C'_{66} = 19.2$ GPa.

Several previous studies on piezoelectric materials[17,18] show that Brillouin spectroscopy is a powerful method to determine the elastic constants of crystals. Brillouin scattering measurements along all the desired crystallographic directions can be made using a given single crystal. In addition, Brillouin measurements can be performed at high temperature because of the non-contact nature of measurements. In the present work, we report the first experimental determination of the elastic constants of $GaAsO_4$ at room temperature and the study of thermal evolution of the elastic constant C_{11} by Brillouin spectroscopy up to 1137 K.

The elastic constants and partial electronic charges were calculated theoretically allowing us to confirm and predict specific properties of $GaAsO_4$ at 0 K. The theoretical model is also applied for the other materials in the quartz group, and the properties are compared with previous experimental values.

2. Experimental Section

2.1. Growth of $GaAsO_4$ Single Crystal and Specimen Preparation. The $GaAsO_4$ crystal used in the present work was prepared by a hydrothermal method in a poly(tetrafluorethylene) (PTFE) lined autoclave as described previously.[11] The $GaAsO_4$ crystal shown in Figure 1 was transparent and colorless. Crystallographic orientations of the crystal were determined by X-ray diffraction using Mo-$K\alpha$ X-rays on an Enraf-Nonius CAD4 diffractometer. It was cut in a $2 \times 2 \times 2$ mm cube having *X* $(2\bar{1}0)$, *Y* (010), and *Z* (001) faces. These faces are perpendicular to the direction of acoustic wave propagation along Cartesian *x* [100], *y* [010], and *z* [001] directions, respectively. We will use the convention of Cartesian directions unless stated explicitly. The crystal was oriented by back scattering X-ray Laue diffraction with an angular accuracy of $\pm 0.3°$. The sample was cut with a

(3) Grimm, H.; Dorner, B. *J. Phys. Chem. Solids* **1975**, *36*, 407.
(4) Kihara, K. *Eur. J. Mineral.* **1990**, *2*, 63–77.
(5) Philippot, E.; Goiffon, A.; Ibanez, A.; Pintard, M. *J. Solid State Chem.* **1994**, *110*, 356.
(6) Philippot, E.; Palmier, D.; Pintard, M.; Goiffon, A. *J. Solid State Chem.* **1996**, *123*, 1.
(7) Philippot, E.; Armand, P.; Yot, P.; Cambon, O.; Goiffon, A.; McIntyre, G. J.; Bordet, P. *J. Solid State Chem.* **1999**, *146*, 114.
(8) Haines, J.; Chateau, C.; Léger, J. M.; Marchand, R. *Ann. Chim. Sci. Mater.* **2001**, *26*, 209.
(9) Haines, J.; Cambon, O.; Philippot, E.; Chapon, L.; Hull, S. *J. Solid State Chem.* **2002**, *166*, 434.
(10) Haines, J.; Cambon, O.; Hull, S. *Z. Kristallogr.* **2003**, *218*, 193.
(11) Cambon, O.; Yot, P.; Rul, S.; Haines, J.; Philippot, E. *Solid State Sci.* **2003**, *5*, 469.
(12) Cambon, O.; Haines, J. *Proceedings of the 2003 IEEE International Frequency Control Symposium & 17th European Frequency and Time Forum*, Tampa, FL, May 8, 2003; IEEE: Piscataway, NJ, 2003; p 650.
(13) Haines, J.; Cambon, O.; Astier, R.; Fertey, P.; Chateau, C. *Z. Kristallogr.* **2004**, *219*, 32.
(14) Haines, J.; Cambon, O. *Z. Kristallogr.* **2004**, *219*, 314.
(15) Cambon, O.; Haines, J.; Fraysse, G.; Détaint, J.; Capelle, B.; Van der Lee, A. *J. Appl. Phys.* **2005**, *97*, 074110.
(16) Cady, W. G. *Piezoelectricity*; McGraw-Hill Book Company: New York, 1946; p 308.
(17) Magneron, N.; Luspin, Y.; Hauret, G.; Philippot, E. *J. Phys. I France* **1997**, *7*, 569.
(18) Armand, P.; Beaurain, M.; Rufflé, B.; Menaert, B.; Papet, P. *Inorg. Chem.* **2009**, *48*, 4988.

wire saw and polished on a Logitech precision polishing machine PM5. The final orientation was controlled with conoscopic interference patterns, that is, by an optical microscopy observation under convergent polarized monochromatic light (Figure 1).

2.2. Brillouin Spectroscopy and Determination of Elastic Constants. The Brillouin measurements were performed using a 2×3 pass Fabry−Perot interferometer in tandem, following Sandercock's design.[19] The incident light ($\lambda = 532$ nm) was obtained from a diode laser. The spacing between the mirrors of the interferometer was fixed at 2.5 mm for room temperature measurements on the X, Y, and Z faces. Such experimental conditions result in a free spectral range (i.e., accessible frequency range) equal to 60 GHz, with a fine resolution of about 100 (or an energy resolution (ΔE) (half width) of about 0.3 GHz). Increased mirror spacing (3.75 mm) was used for high temperature measurements of C_{11} to decrease the free spectral range to 40 GHz to focus on the C_{11} Brillouin peak. Backscattering geometry was used. We measured either the scattered light with the same polarization as the incident light (vertical/vertical VV polarization) or the scattered light with a polarization lying at 90° from that of the incident light (VH or vertical/horizontal). A Linkam TS 1500 heating stage was used to perform high temperature Brillouin experiments. The Linkam TS was calibrated by measuring the temperature of a thermocouple placed between two quartz plates at the sample position. At each temperature step, the sample temperature was allowed to equilibrate with the heating stage for 5−10 min. Acquisition time for each spectrum was 300 s.

3. Theoretical Calculations

Calculations were performed using the CRYSTAL06[20] package developed in Torino. The crystalline orbitals are expanded in terms of a localized atomic Gaussian basis set, in a way similar to the LCAO (linear combination of atomic orbitals) method currently adopted for molecules. The eigenvalues equations are solved using three sets for Density Functional Theory (DFT) calculations:

- Becke's three parameter adiabatic connection exchange functional[21] in combination with the Lee−Yang−Parr correlation functional,[22] noted B3LYP,
- The local density approximation using Dirac−Slater exchange functional (LSD)[23] and Vosko−Wilk−Nusair correlation functional (VWN),[24] known as LDA,
- the non local GGA (generalized gradient approximation) approach developed on the Perdew−Burke−Ernzerhof functionals,[25] referenced as PBE.

The number of k points in the first irreducible Brillouin zone in which the Hamiltonian matrix was diagonalized is 34.

All electron basis sets were used for oxygen (8−411(11)) and gallium (8−64111(41)) for orbital expansion solving the Kohn−Sham equation iteratively. To reduce the computational cost, Durand and Barthelat effective core pseudopotentials (ECP)[26] were used to model the core electrons in arsenic (PS-21(1)).[27] Tolerances on total energy in the iterative resolution process are set to accurate values of 10^{-10} hartree. The level of accuracy in evaluating the Coulomb series is controlled by five parameters, for which standard values given in CRYSTAL (i.e., 6 6 6 6 12) have been used. Vibration frequency analysis was performed to guarantee that optimized structures are local minima for each set of DFT calculations. The refractive index η^{∞} (components $xx = yy$, zz, and average) was calculated within the CPHF-(KS) approach,[28,29] where ∞ denotes electronic contribution only, that is, static values of electric field without ionic relaxation effect. To be compared with experimental value, the wavelength λ must be taken into account. For η^{λ} we used a version of CRYSTAL under development (see Acknowledgments).

For the determination of elastic coefficients, the non-zero independent components of the elastic tensor have been computed by fitting the total energy as a function of the applied strain. We consider 11 values for the strain in the interval $[-0.030; +0.030]$ for the fitting at a constant volume.

4. Results and Discussion

4.1. Determination of Refractive Index and Elastic Constants at Room Temperature. The frequency shift of the Brillouin lines allows one to determine the velocity of elastic waves traveling through the crystal. $GaAsO_4$ belongs to the family of α-quartz materials, space group $P3_121$ or $P3_221$. According to its point group, it has six independent elastic moduli C_{11}, C_{33}, C_{44}, C_{66}, C_{13}, and C_{14}. These elastic constants except C_{13} are related with longitudinal (L) and transverse (T) acoustic phonon modes in the X, Y, and Z directions. Because of the crystal cut of the sample and the geometry of the measurement (use of a Linkam heating stage without any goniometer holder), it was impossible to measure the C_{13} elastic constant. In the simplest case, the elastic wave velocity V is related to elastic constants C_{ii} of the crystal by

$$C_{ii} = \rho V^2 \qquad i = 3,\ 4, \tag{1a}$$

where ρ is density (4.23 g cm^{-3} for $GaAsO_4$) and C_{33} (C_{44}) corresponds to L (T) mode vibrations propagating along [001] direction. A more complex relationship exists when the piezoelectric correction has to be taken into account

$$C_{ii} = \rho V^2 - e_{11}^2/\varepsilon_{11} \qquad i = 1,\ 6 \tag{1b}$$

where e_{11} and ε_{11} are the components of piezoelectric stress and dielectric permittivity tensors, respectively. C_{11} and C_{66} correspond respectively to L vibrations propagating along the [100] direction and T vibrations propagating along [010].

(19) Sangwal, K.; Kucharczyk, W. *J. Phys. D* **1987**, *20*, 522.
(20) Dovesi, R.; Saunders, V. R.; Roetti, C.; Orlando, R.; Zicovich-Wilson, C. M.; Pascale, F.; Civalleri, B.; Doll, K.; Harrison, N. M.; Bush, I. J.; D'Arco, Ph.; Llunell, M. *CRYSTAL06 User's Manual*; University of Torino: Torino, Italy, 2006.
(21) Becke, A. D. *Phys. Rev. A* **1988**, *38*, 3098.
(22) Lee, C.; Wang, W.; Parr, R. G. *Phys. Rev. B* **1988**, *37*, 785.
(23) Dirac, P. A. M. *Proc. Cambridge Phil. Soc* **1930**, *26*, 376.
(24) Vosko, S. H.; Wilk, L.; Nusair, M. *Can. J. Phys* **1980**, *58*, 1200.
(25) Perdew, J. P.; Burke, K.; Ernzerhof, M. *Phys. Rev. Lett.* **1996**, *77*, 3865.
(26) Durand, P.; Barthelat, J. C. *Theor. Chim. Acta* **1975**, *38*, 283.
(27) Labéguerie, P.; Harb, M.; Baraille, I.; Rérat, M. *Phys. Rev. B* **2010**, *81*, 045107.
(28) Ferrero, M.; Rérat, M.; Orlando, R.; Dovesi, R.; Bush, I. J. *J. Phys. Conf. Series* **2008**, *117*, 12016.
(29) Ferrero, M.; Rérat, M.; Orlando, R.; Dovesi, R. *J. Comput. Chem.* **2008**, *29*, 1450.

Table 1. Acoustic Mode Frequency, Line Width and Elastic Constant from Brillouin Spectroscopy of a $GaAsO_4$ Single Crystal

		Brillouin line parameter (GHz)		
geometry	expression of ρV^2	frequency shift	width	elastic constant (GPa)
X [100] L	$C_{11} + e_{11}^2/\varepsilon_{11}$	23.299(5)	0.31(2)	C_{11}: 59.32(3)
Y [010] T	$C_{66} + e_{11}^2/\varepsilon_{11}$	13.23(1)	0.31(4)	C_{66}:19.12(5)
Y [010] PL	$(C_{44} + C_{11})/2 + [(C_{44} - C_{11})^2 + 4C_{14}^2]^{1/2}/2$	23.12(1)	0.32(2)	C_{14}[#]: 1.7(5)
Y [010] PT	$(C_{44} + C_{11})/2 - [(C_{44} - C_{11})^2 + 4C_{14}^2]^{1/2}/2$	16.74(1)	0.30(5)	
Z [001] L	C_{33}	30.783(6)	0.35(2)	C_{33}:103.54(3)
Z [001] T	C_{44}	16.76(1)	0.26(3)	C_{44}: 30.70(3)

[#] Calculated using [010] PT mode.

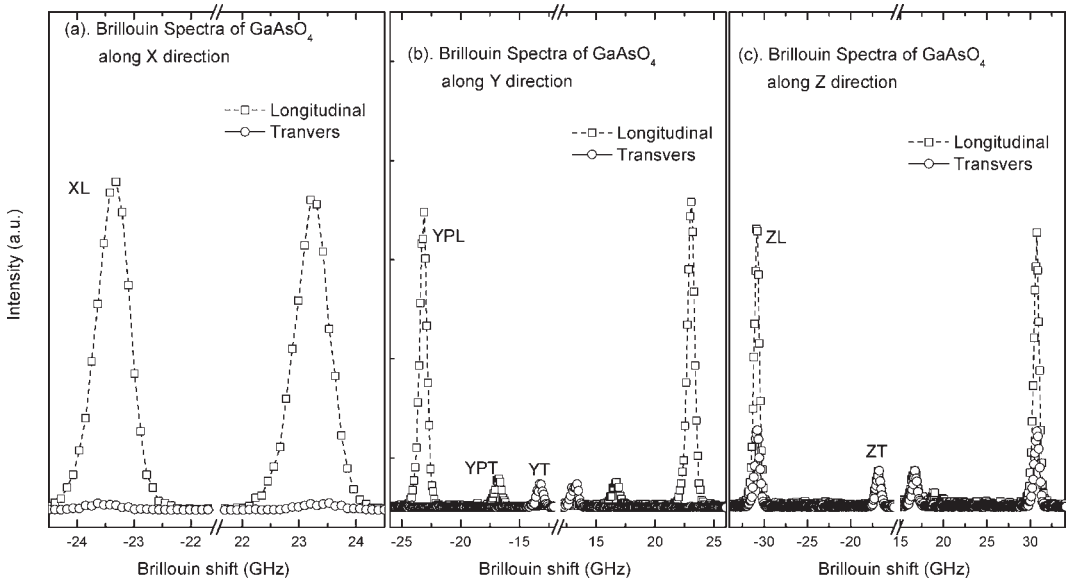

Figure 2. Brillouin scattering from the acoustic modes along the (a) x [100], (b) y [010], and (c) z [001] directions of a hydrothermally grown α-quartz type $GaAsO_4$ single crystal. Solid and dotted lines represent the transverse and longitudinal mode spectra, respectively.

The Brillouin frequency shift ν_B which is the shift in the frequency of light of incident wavelength λ, is related (in backscattering geometry) with V by

$$V = \lambda \nu_B/(\eta_0 + \eta_e) \qquad (2)$$

where η_o and η_e are ordinary and extraordinary refractive indices, respectively.

The refractive index of $GaAsO_4$ was experimentally measured using a classical refractometer equipped with a sodium lamp (λ = 589.3 nm) and was found to be 1.66. The correction of the refractive index for the wavelength used in the present experiments (λ = 532 nm) is expected to be about 0.005, based on results obtained for $GaPO_4$.[30] The average experimental value 1.655 of the refractive index $(\eta_o+\eta_e)/2$ for $GaAsO_4$ after correcting for the shift in wavelength was used in elastic constant calculations. This value is in very good agreement with the value 1.65 ± 0.02 derived from value of C'_{66} = 19.2 GPa, measured by the piezoelectric frequency resonance method.[15]

The elastic constant C_{12} depends on other independent elastic constants and can be calculated as follows: $C_{12} = C_{11} - 2C_{66}$.

The measured value[11] of dielectric constant ε_{11} is 8.5 $\varepsilon_0 Fm^{-1}$, where ε_0 is the permittivity of vacuum. The experimental value of e_{11} from direct piezoelectric measurements is not available in the literature. However, it can be observed from previous work that the piezoelectric correction is usually small, of the order of 2%.[18,31] Theoretical calculations confirm the estimation of this correction. The piezoelectric tensor of $GaAsO_4$ has been obtained previously by Labéguerie et al.,[27] using B3LYP calculations with two independent components, e_{11} = 0.20 C/m^2 and e_{14} = 0.17 C/m^2. Using e_{11} = 0.20 C/m^2 and the experimental value of $\varepsilon_{11} = 8.5\varepsilon_0 Fm^{-1}$, $e_{11}^2/\varepsilon_{11}$ is found to be 0.53 GPa. This correction represents only 0.9% of experimental C_{11} = 59.32 GPa, and confirms that piezoelectric correction can be neglected. Therefore, as in previous studies,[32] we do not consider the piezoelectric correction in the present work. The other independent elastic constant C_{14} can be obtained from quasi-longitudinal (QL) and quasi-transverse (QT) modes propagating perpendicular to the Y face (table 1).

Brillouin scattering spectra of the L and T modes from the three faces of the $GaAsO_4$ are shown in Figure 2. Quasi-longitudinal (QL) and quasi-transverse (QT) modes are not pure modes and are observed in the VV geometry (for the longitudinal mode) spectra from the Y face. These Stokes and antiStokes modes could be

(30) Defregger, S.; Engel, G. F.; Krempl, P. W. *Phys. Rev. B* **1991**, *43*, 6733.

(31) Wallnöfer, W.; Krempl, P. W.; Asenbaum, A. *Phys. Rev. B* **1994**, *49*, 10075.

(32) Grimsditch, M.; Polian, A.; Brazhkin, V.; Balitskii, D. *J. Appl. Phys.* **1998**, *83*, 3018.

Table 2. Ab initio Calculations of Structural Parameters, Refractive Index and Elastic Constants for $GaAsO_4$ at 0 K Compared to Experimental Results at 298 K

DFT set	LDA	PBE	B3LYP	exp. (298 K)
a (Å)	4.7922(4.1%)	4.9980(0.02%)	5.0755(1.6%)	4.997[7]
c (Å)	11.3356(0.4%)	11.5684(1.6%)	11.5475(1.4%)	11.386[7]
c/a	2.3654(3.8%)	2.3146(1.6%)	2.2751(2.3%)	2.2786[7]
Ga−O−As angle (deg)	121.7(6.1%)	125.5(3.2%)	129.9(0.2%)	129.6[7]
δ (deg)	32.8(22%)	30.1(12%)	27.0(0.4%)	26.9[7]
ΔE_g (Γ) (eV)	3.51	3.33	5.68	
$\eta_{xx}^{\infty} = \eta_{yy}^{\infty}$; η_{zz}^{∞}	1.7763 ; 1.8574	1.7233 ; 1.8029	1.6053 ; 1.6723	
$\overline{n}^{\infty}$	1.8033	1.7498	1.6276	
$\eta_{xx}^{589.3\ nm} = \eta_{yy}^{589.3\ nm}$; $\eta_{zz}^{589.3\ nm}$	1.8186 ; 1.9002	1.7655 ; 1.8623	1.6275 ; 1.6954	
$\overline{n}^{589.3\ nm}$	1.8458(11%)	1.7978(8.3%)	1.6501(0.6%)	1.660
$\eta_{xx}^{532\ nm} = \eta_{yy}^{532\ nm}$; $\eta_{zz}^{532\ nm}$	1.8301 ; 1.9128	1.7770 ; 1.8748	1.6330 ; 1.7015	
$\overline{n}^{532\ nm}$	1.8577(12%)	1.8076(9.2%)	1.6558(0.05%)	1.655
C_{11} (GPa)	46.7(21%)	52.2(12%)	60.7(2.3%)	59.32(3)
C_{12} (GPa)	43.4(105%)	21.0(0.5%)	18.6(12%)	21.1(1)
C_{13} (GPa)		21.6	22.7	
C_{14} (GPa)	4.8(182%)	1.1(35%)	−2.8 (n.s.)	1.7(5)
C_{33} (GPa)	124.0(25%)	100.9(1.7%)	95.4(7.9%)	103.54(3)
C_{44} (GPa)	17.0(45%)	23.7(22%)	28.1(8.5%)	30.70(3)
C_{66} (GPa)	1.7(91%)	15.6(18%)	21.0(9.8%)	19.12(5)

observed symmetrically around a strong (truncated) central Rayleigh line. The *X*-face does not exhibit any transverse mode, which is as expected for quartz type materials. The important parameters in the Brillouin spectra are the frequency shift and line width, from which the elastic constant and disorder are measured, respectively. Although the shape of Brillouin lines can be fit with a single Gaussian rather than a mixed shape, such a fit was not performed as it is nonphysical. The Brillouin line width has contribution from intrinsic damping processes within the specimen and an instrumental broadening, which are approximately of Lorentzian and Gaussian type, respectively. The Lorentzian part of the line width was deconvoluted from Voigt peak fit profile keeping the Gaussian component fixed to the instrumental broadening. The instrumental broadening was obtained from the width of the laser line without any scatterer. The frequency shift and width of the Brillouin lines are shown in Table 1. Elastic constants extracted from the peak positions using eqs 1 and 2 are also summarized in Table 1. The value of C_{66} (19.12 GPa) is in a good agreement between with that measured by piezoelectric measurements (19.2 GPa) on *Y* rotated cut with a cut angle of about −6.3°.[15] C_{12} can be calculated from the experimental values: $C_{12} = C_{11} - 2C_{66} = 21.1(1)$ GPa. Other elastic constants determined experimentally are being reported for the first time in the present work.

Theoretical results of refractive index are in very good agreement with the experimental ones. As expected, for the three kinds of DFT Hamiltonians (Table 2) $\eta\infty$ is lower than $\eta^{589.3\ \mathrm{nm}}$ and lower than $\eta^{532\ \mathrm{nm}}$, because of a normal dispersion curve. At 589.3 nm (sodium lamp) and 532 nm, B3LYP gives 1.6501 (deviation of 0.6% compared to the experimental value 1.66) and 1.6558 (deviation of 0.05% compared to 1.655), respectively. B3LYP leads to better results than LDA and PBE to describe electronic properties such as dielectric constant and refractive index depending strongly on electronic gap value. Where LDA and PBE functionals always underestimate the gap, the B3LYP hybrid functional is known to give a well-estimated value (experimental gap is missing here).

The results of ab initio calculations of the elastic constants for $GaAsO_4$ are shown also in Table 2. These agree well with corresponding experimental values. We must note that in all ab initio calculations, temperature is not taken into account, so we must compare these as an extrapolation to 0 K of experimental data. That is why no thermal evolution for C_{11} could be performed. Nevertheless, extrapolation of experimental values of C_{11} values to 0 K gives a good agreement with the theoretical B3LYP value of 60.7 GPa (see section 4.2). Except for low experimental values of (C_{12}) and (C_{14}), for which measurements have also large relative error, the deviation does not exceed 10%. Note that the change of sign obtained for C_{14} with the different Hamiltonians indicates a very low value for this component. Calculations are thus an efficient way to predict properties of materials that are difficult to measure.

It is useful to compare the elastic constants of $GaAsO_4$ with the values obtained for other piezoelectric crystals of the same family.[17,31−33] Figure 3 represents the variation of elastic constants of these materials in terms of the cell parameter c/a ratio. The c/a ratio represents overall distortion of the structure. The c/a ratio for SiO_2 and GeO_2 has been multiplied by 2 to compare with the ABO_4 type materials, in the following discussion. In the ABO_4 type materials, the *c*-dimension of the trigonal unit cell is two times that of the AO_2 type materials because of ordering of the *A* and *B* atoms in the corner-sharing tetrahedra. Some of the structural parameters better represent the distortion of the structure locally, as discussed in a review by Philippot et al.[6] Using a parameter which represents local distortion would not be appropriate here because the scattering vector involved in Brillouin spectroscopy is short as compared to the reciprocal lattice vector. The c/a ratio for ideal (undistorted) quartz structure is 2.196 (β-quartz) and increases from 2.2 for α-SiO_2 to 2.28 for $GaAsO_4$. The larger this parameter, the more distorted is the structure.

(33) James, B. J. *Proceedings of the 42nd Annual Frequency Control Symposium*, Baltimore, MD, June 1−3, 1988; IEEE: New York, 1988; p 146.

Similar behavior is observed for the AO_2 and ABO_4 type materials. The most significant difference between these two subgroups in the quartz type materials is that the C_{33} of the ABO_4 compounds is 17% lower than those of the AO_2 type materials. It has been previously observed that the evolution of distortion among the quartz homeotypes differs slightly, depending on the difference in volume of the neighboring tetrahedra.[7] In case of SiO_2 and GeO_2, the neighboring tetrahedra are of identical volume, in contrast to the ABO_4 materials (except for $AlAsO_4$, for which Al−O and As−O bond distances are comparable and it behaves like A_2O_4). The evolution of elastic constants as seen in the present work corroborates such a difference. This will be further discussed in conjunction with the role of chemical bonding in the neighboring tetrahedra (section 4.3). Nevertheless, the evolution of the elastic constants has to be correlated to the structural distortion described by the tetrahedral tilt angle (δ) in the quartz-type materials, which is the order parameter for the $\alpha-\beta$ transition and usually used to describe the structural distortion.[3,14]

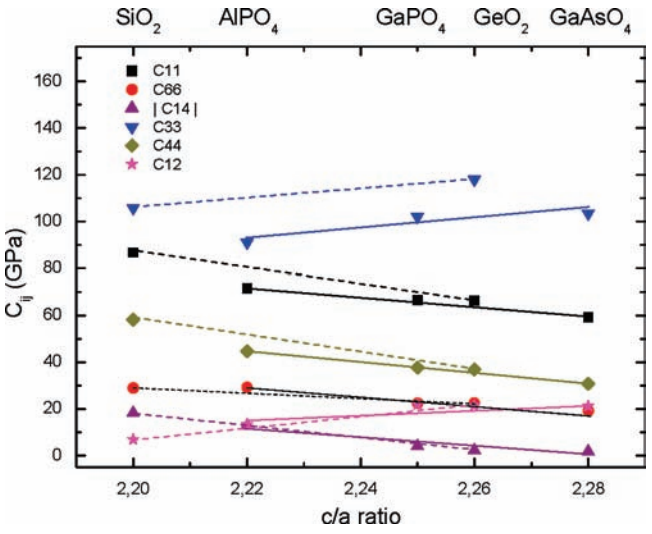

Figure 3. Elastic constants of $GaAsO_4$ and other α-quartz hometoptypes.[17,20,31,32] The c/a ratio has been used to represent the structural distortion (c/a ratio for SiO_2 and GeO_2 are twice to their true values to compare with the ABO_4 type materials for which the c-dimension of unit cell is doubled as compared to the AO_2 type materials).

Reduction in pure elastic moduli C_{11}, C_{66}, and C_{44} indicates softening of the structure in the direction perpendicular to the c-axis. On the other hand, the elastic constant C_{33} along the c-axis increases with the degree of the distortion. This indicates a dynamic asymmetry in and normal to the c-axis. The stiffness increases along the c-axis whereas it decreases in the xy plane as the structural distortion increases in AO_2 type materials (from SiO_2 to GeO_2) and in ABO_4 materials (from $AlPO_4$ to $GaAsO_4$). This can be related to the increase of c/a as a function of δ as reported in pressure and temperature studies.[14]

The behavior of materials, as revealed from the evolution of elastic constants among the quartz homeotype materials, shows concordance with the behavior studied by other techniques. High pressure studies on quartz type materials show that the compressibility is greater in the xy plane than along the c-axis.[6,14,34] This indicates that the lattice is softer in the plane perpendicular to the c-axis to accommodate static changes. The same argument could be applied for dynamical fluctuations caused by elastic waves. The higher value of C_{33} with respect to C_{11} for $GaAsO_4$ is in agreement with this behavior, highlighting the dynamic softness within the xy plane as compared to the relatively stiffer interplane interaction. This difference can be related to the intrinsic distortion of the piezoelectric materials. To confirm this, it would be interesting to compare the ratios of these two elastic constants with other parameters (c/a ratio, ρ, θ, and δ). These parameters are quantitative measures of the asymmetry between c-axis and directions perpendicular to it. Increasing distortion in an ABO_4 type material is microscopically characterized by a reduction in the bridging angle θ. Greater distortion results in a decreased value of this angle, and expansion of the unit cell along the c-axis.[3] The relative behavior of the material-response along and perpendicular to the xy plane can be represented by the ratio C_{33}/C_{11} of elastic constants. In Figure 4 the known distortion parameters are summarized for quartz analogues in terms of the parameter C_{33}/C_{11}. The linear correlation of the structural distortion parameters with the ratio of elastic constants is a direct evidence of structural-physical

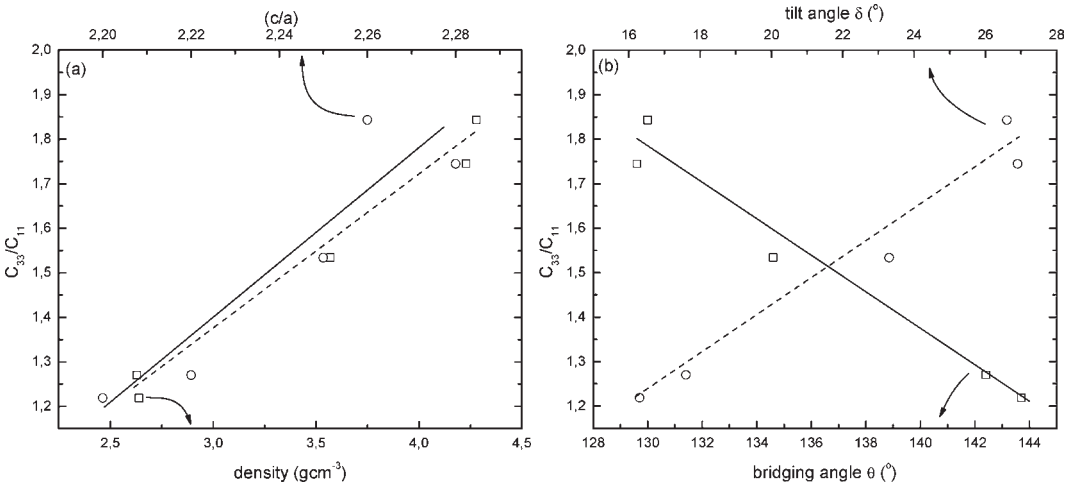

Figure 4. Variation of C_{33}/C_{11}, the ratio of elastic constants, along c- and a-axis with the standard parameters characterizing the structural distortion: (a) density[14](squares) and c/a ratio (circles); (b) intertetrahedral bridging-angle θ (squares) and tilt angle δ (circles).

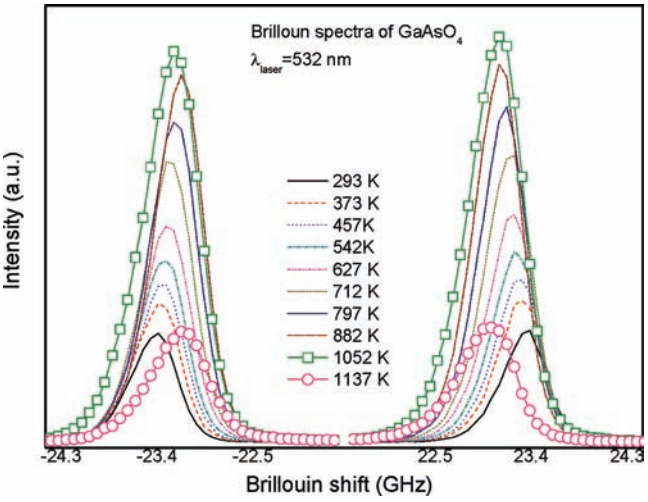

Figure 5. Temperature dependent Brillouin backscattering spectra of the acoustic mode along [100] direction for a $GaAsO_4$ single crystal. The region between the Stokes and anti-Stokes lines is excluded to better observe the relative shift of the acoustic wave frequency.

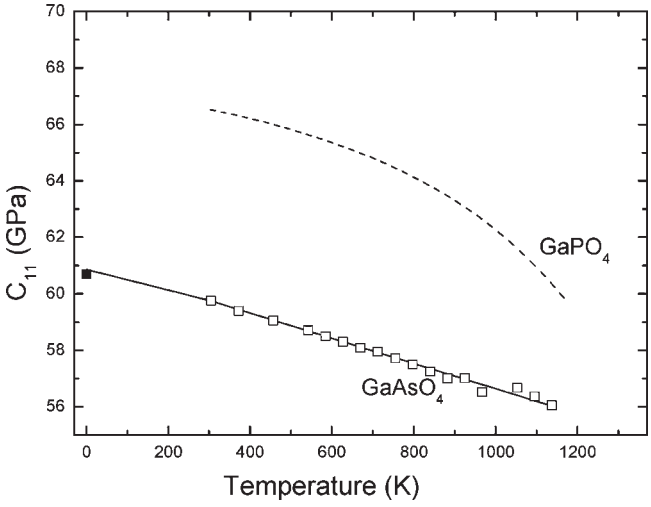

Figure 6. Variation of C_{11} of $GaAsO_4$ with temperature (symbols) and linear fit (solid line) to data (symbols). Thermal variation of C_{11} for $GaPO_4$[18] is shown for comparison (dashed line).

property relationships. In addition, it provides a new parameter, which could be directly used to evaluate the piezoelectric response of a material.

The structural anisotropy essentially results from chemical anisotropy, discussed in more detail in relation to the distortion in SiO_2.[3] It means that there is a difference in the electron density distribution or the effective bond order in these two directions.

4.2. Thermal Behavior of Elastic Constant C_{11}. Pressure and temperature have a significant effect on the properties of solids. Not only the dimensions and volume of the unit-cell but also the structural distortions are sensitive to these thermodynamic variables.[6,14] An important property of a piezoelectric material from the point of view of potential applications is its thermal stability. C_{11} shows the most interesting behavior among all elastic constants of being most susceptible to softening in the xy plane and because of changes in the degree of structural distortion. We therefore investigated the thermal behavior of C_{11}. Figure 5 shows Brillouin spectra of the L mode propagating along the [100] direction. At 1137 K, the peak intensity decreases because of decomposition at the surface of the sample. The temperature dependence of the density was obtained from the unit-cell volume obtained from variable temperature X-ray diffraction experiments.[15] These values were fitted with a third order polynomial to calculate density at desired temperatures for the Brillouin experiments. The elastic constant values are given versus temperature in Table 3. The general behavior of decreasing elastic constant C_{11} with increasing temperature (Figure 6) is in agreement with other quartz type materials, for example quartz,[35] $AlPO_4$[17] and $GaPO_4$.[18] For comparison, we also plot the temperature dependence of C_{11} for $GaPO_4$ in Figure 6. The slope dC_{11}/dT of the curves (Figure 6) at room temperature is found to be -3.6 (6) $\times 10^{-3}$ and -2.8×10^{-3} GPa K^{-1} for $GaAsO_4$ and $GaPO_4$,[18] respectively. The coefficients T_i (i = 1, 2, 3, 4)

Table 3. Elastic Constant C_{11} Determined from Brillouin Spectroscopy on a $GaAsO_4$ Single Crystal

temperature (K)	C_{11} (GPa)
293	59.75(3)
373	59.40(3)
457	59.05(2)
542	58.71(2)
584	58.51(2)
627	58.31(2)
670	58.09(2)
712	57.95(2)
754	57.72(2)
797	57.49(2)
840	57.25(2)
882	57.01(2)
925	57.02(2)
967	56.52(2)
1052	56.68(2)
1095	56.37(3)
1137	56.05(3)

of a fourth-degree polynomial expression

$$\frac{\Delta C_{11}}{C_{11}(T_0)} = T_1\Delta T + T_2(\Delta T)^2 + T_3(\Delta T)^3 + T_4(\Delta T)^4$$

represents the thermal behavior of C_{11}.[18] This expression is based on a Taylor series expansion. Here, Δ represents the difference of corresponding quantities at temperature T and room temperature T_0. Only the first term in the expansion is needed for $GaAsO_4$ and $T_1 = -6.36$ (8) $\times 10^{-5}$ K^{-1}. On comparing this value with those (-42.41×10^{-6} K^{-1}, -61.47×10^{-9} K^{-2}, 43.97×10^{-12} K^{-3}, and -82.46×10^{-15} K^{-4}) of $GaPO_4$, it can be seen that although the room temperature stability of $GaAsO_4$ is not better than that of $GaPO_4$, it is far superior at higher temperature.

The distinct behavior of $GaAsO_4$ is easy to observe. The minor variation of C_{11} in $GaAsO_4$ is in sharp contrast to a strong decrease in elastic constant (sound velocity) observed for other quartz isotypes close to the highest temperature for the α phase (because of limitation from α–β transition, transition to a β-cristobalite form or thermal decomposition). The decrease in Brillouin line

(34) Levien, L.; Prewitt, C. T.; Weidner, D. J. *Am. Mineral.* **1980**, *65*, 920.
(35) Carpenter, M. A.; Salje, E. K. H.; Graeme-Barber, A.; Wruck, B.; Dove, M. T.; Knight, K. S. *Am. Mineral.* **1998**, *83*, 2.

frequency from room temperature is about 12, 3, and 1.2% for α-quartz,[36] $GaPO_4$[18] and $GaAsO_4$ (this work), respectively. These values correspond to the temperature of about 843, 1133, and 1137 K, respectively. The high thermal stability is an intrinsic structural property of $GaAsO_4$, which is highly distorted and far from the β-quartz-type structure. This is because higher energy is required to tilt adjacent tetrahedra to accommodate thermally induced strain in the lattice and ultimately to obtain $\alpha-\beta$ phase transformation.

The Brillouin line-width is indicative of damping in the elastic mode propagation. We observed in the present temperature dependent experiment that the line-width seems to be almost invariant up to about 967 K beyond which it increases with temperature. The deconvoluted line width (~0.25 GHz) below this temperature was comparable to the experimental resolution (0.25 GHz); hence, quantitative analysis was not made. This produces for an uncertainty of about 3% in absolute determination of elastic constants at room temperature. The error in the relative behavior of C_{11} with temperature was principally due to the uncertainty in Brillouin peak position (about 0.01 GHz) from the fitting routine which is of the order of 0.2%. Quantitative Brillouin measurements were limited to a temperature less than 1173 K because of decomposition of the material at the surface above this temperature.

4.3. Piezoelectricity and Bond Polarizabilities in $GaAsO_4$. A previous study carried out by Cambon et al[37] emphasizes the role of individual cation-oxygen bond polarizabilities on the structural distortion in α-quartz homeotypes. The cation-oxygen bond polarizability increases with increasing size of the cation. An additional electronic shell of d-electrons results in the large increase in the radii of atoms. If we see in the perspective of increasing distortion from $AlPO_4$, $GaPO_4$, and $GaAsO_4$, the covalent radii of Al, Ga and P, As are 1.18, 1.26 and 1.06, 1.19 Å. Thus, among the piezoelectric materials (ABO_4) having quartz structure, $GaAsO_4$ has the largest cations (A = Ga and B = As). The size of the cation can affect the thermal behavior of the material. From the structural point of view, ABO_4 type materials having a quartz-type structure are built up of corner sharing tetrahedra of oxygen atoms. The tetrahedral void is filled with a suitable cation (A and B alternatively). It is then expected that the large cations (Ga and As) in $GaAsO_4$ which give rise to longer bond lengths and smaller intertetrahedral bridging angles would create more steric hindrance to tilting the tetrahedral framework as a function of thermodynamic variables (temperature and/or pressure). The cation size also modifies the piezoelectric coupling coefficient k of the crystal, which is controlled at the microscopic scale by bond polarizability. Materials having more polarizable bonds will be expected to have higher values of k. In $Ga_xAl_{1-x}PO_4$,[37] the cation-oxygen bond polarizability increases with increasing size of the cation. Similarly, the bonds in $GaAsO_4$ can be expected to be more covalent in nature because of their higher polarizability. This is consistent with a high piezoelectric coupling coefficient in $GaAsO_4$ (~21% at room temperature), which we can expect to be stable with temperature because of the stability of the structure.

Table 4. Calculated Partial Charges in ABO_4 α-Quartz Type Materials by Using the B3LYP Set for DFT Calculations

ABO_4	$AlPO_4$	$GaPO_4$	$GaAsO_4$
	A^{+III}		
Al	+1.91		
Ga		+1.62	+1.57
	B^{+V}		
P	+2.36	+2.12	
As			+0.9
	O^{-II}		
O1	−1.062	−0.927	−0.633
O2	−1.071	−0.945	−0.602

Table 5. Structural Distortion and Piezoelectric Properties in the α-Quartz Homeotypes[a]

	AO_2 type		ABO_4 type		
materials	SiO_2[33]	GeO_2[9,32]	$AlPO_4$[39]	$GaPO_4$[31]	$GaAsO_4$[11,15]
θ (°)	143.2	130.22	142.4	134.2	129.6
C_{11} (GPa)	86.79	66.4	69.3	66.58	59.3
d_{11}(pC/N)	2.31	4.1	3.3	4.5	
ε_{11}	4.45	7.43	4.73	5.2	8.5

[a] d_{11} for $GaAsO_4$ is not measured.

The B3LYP set has been also used to calculate the partial charges in $GaAsO_4$ and for other ABO_4 α-quartz-type materials (Table 4). For the both $AlPO_4$ and $GaPO_4$ materials, these theoretical values are in a good agreement with the previous experimental partial charges already published.[37] In the ABO_4 α-quartz-type materials we observe a decrease of the partial charges with increasing cation size indicating the more covalent nature of the chemical bond. We can note also that this effect is more marked when the size of the B cation is increased: the partial charge decreases from +2.36 to +0.9 when we replace P by As. This shows that there is a link between the network distortion and the bond polarizability. Recently Wilson and Salmon[38] have intvestigated network-forming tetrahedral glasses. They found that the network topology is controlled by varying the anion polarizability, which similarly governs the interterahedral bond angle.

4.4. Piezoelectric Properties in the α-Quartz Isotypes. Dielectric (ε^T, ε^S), elastic (C^E, s^E) and piezoelectric constants (d, e)[16] can be compared for all α-quartz isotypes in relation with the structural distortion (Table 5). Knowing that the coupling factor is classically expressed by

$$k = \frac{d}{\sqrt{\varepsilon^T s^E}} \quad \text{or} \quad \frac{e}{\sqrt{\varepsilon^S C^E}}$$

it is evident that coupling coefficient is improved by increasing the piezoelectric constant and decreasing the elastic constant. Along the x-axis, the elastic constant C_{11}

(36) Shapiro, S. M.; Cummins, H. Z. *Phys. Rev. Lett.* **1968**, *21*, 1578.
(37) Cambon, O.; Haines, J.; Cambon, M.; Keen, D. A.; Tucker, M. G.; Chapon, L.; Hansen, N. K.; Souhassou, M.; Porcher, F. *Chem. Mater.* **2009**, *21*, 237.
(38) Wilson, M.; Salmon, P. *Phys. Rev. Lett.* **2009**, *103*, 157801.
(39) Bailey, D. S.; Andle, J. C.; Lee, D. L.; Soluch, W.; Vetelino, J. F.; Chai, B. H. T. *Ultrason. Symp.* **1983**, 335.

is the lowest for $GaAsO_4$. $GaAsO_4$ should exhibit the highest value for the piezoelectric constant d_{11}. The link between chemical nature of atoms, bond polarizability, structural distortion, and piezoelectric properties is now well established. $GaAsO_4$ exhibits the highest polarizability with the highest degree of distortion and the lowest elastic constant in the *xy* plane. The measurement of physical constants confirms that $GaAsO_4$ is the best piezoelectric material in the α-quartz group with a very good thermal stability.

5. Conclusion

The elastic constants of $GaAsO_4$ have been measured by Brillouin spectroscopy at room temperature for the first time on a single crystal grown by hydrothermal methods. The temperature dependence of the C_{11} elastic constant has been measured by Brillouin experiments to determine the thermal stability of piezoelectric properties. This work provides experimental support for structural-physical properties relationships that predict best piezoelectric properties of $GaAsO_4$ in the quartz family. The existence of large cations in the tetrahedra makes the structure more stable with respect to thermally induced structural distortions. It is important to note the small variation of the elastic constant C_{11} with temperature up to the thermal decomposition temperature of about 1303 K for $GaAsO_4$, which marks the loss of piezoelectric properties at a temperature higher than existing materials of the α-quartz type. The almost linear thermal behavior of $GaAsO_4$ would make it possible to more accurately compensate the temperature effects than any other material of quartz family. Finally, ab initio calculations for this compound yield very similar results for structural and elastic properties as well as for the refractive index.

Acknowledgment. The authors would like to thank the ANR for financial support (Contract No. ANR-07-BLAN0258-PIEZOCRIST). We also acknowledge Mauro Ferrero from the University of Torino, for his help in determination of η^{λ} with a soon to be released version of CRYSTAL.